JOURNAL OF MATERIALS SCIENCE 3 (1968) 178–182

Scanning-Electron-Beam-Excited Charge Collection Micrography of GaAs Lasers

D. B. HOLT, B. D. CHASE
Department of Metallurgy, Imperial College of Science and Technology, London SW7, UK

Received 20 November 1967

The Fabry-Perot mirror faces of a number of Zn-diffused Te-doped GaAs lasers were examined by means of scanning-electron-beam-excited charge collection (SEBECC) micrography. Many lines of subsurface damage due to mechanical polishing were observed. The micrographs of certain lasers contained dark dots and lines surrounded by white areas. These were probably due to segregation of the Te to produce regions of high Te density surrounded by denuded zones. The position and width of the p-n junction region is directly observable under certain conditions in SEBECC micrographs. By the use of double exposure photography, therefore, the relation between irregularities in the p-n junction and defects in the material can be made visible. Etching was used to check the interpretation of the SEBECC micrographs. A qualitative discussion of defect visibility and artefacts in the micrographs is given.

1. Introduction

Electron beams incident upon semiconducting crystals produce five distinct types of effect: secondary electrons, back-scattered electrons, fluorescent X-rays, recombination radiation, and injected charge carriers. The latter can, when a p-n junction is present in the material and contacts are applied to the p- and to the n-type material, give rise to an electrical signal that can be readily detected externally. Each of the five types of effect can be detected, amplified, and used as video signal to give a micrographic map of signal strength on a CRO screen that is scanned in unison with the electron beam scanning the specimen [1]. Thus each type of effect is the basis for a physically distinct type of scanning electron microscopy. Secondary electrons and back-scattered electrons form the basis for scanning electron microscopy as that term is normally used. For this technique the acronym SEM (from the phrase "scanning electron microscopy") has been coined. Fluorescent X-rays give rise to the micrographs obtained in electron probe microanalysis. Scanning-electron-beam-excited (infrared) recombination radiation micrography of GaAs has received considerable attention [1-7]. The acronym SEBERR (from the phrase "scanning-electron-beam-excited recombination radiation) has been coined for this technique. The electrical signal induced in contacts to the p- and n-sides of a semiconducting specimen when an electron beam is incident near a p-n junction, provides the basis for another form of microscopy. This has been exploited to study diffusion-induced dislocations and other defects near p-n junctions in silicon [8-12]. The p-n junctions in these experiments were observed in plan view.

The electrical signal induced in p- and n-side contacts to GaAs lasers with the electron beam incident on the side Fabry-Perot mirror faces, so that the p-n junctions were seen edge-on, was used as video signal to form micrographs in the work reported here. The acronym SEBECC derived from the initial letters of the phrase "scanning-electron-beam-excited charge collection" will be used to designate this technique as no other name has hitherto been used. (SEBECC micrographs have been described as "photoconductive maps" however [13]). It is necessary to use the non-committal term "charge collection" because more than one mechanism can contribute to contrast formation, and the mechanisms may vary from one material and one set of

microscope operating conditions to another.

2. Experimental Methods

The GaAs lasers were kindly supplied by Services Electronics Research Laboratories*. They were produced by the diffusion of Zn at 850° C for 2½ h into Te-doped GaAs grown by the horizontal boat (Bridgman) technique. The mirror faces of these lasers were mechanically polished.

The lasers were examined by the SEBECC technique in a JEOL electron probe microanalyser. To check the interpretation of the SEBECC micrographs, the AB etch developed by Abrahams and Buiocchi [14] was used.

3. Results and Discussion

3.1. Defects in SEBECC Micrographs

A prominent feature of the SEBECC micrographs of all the lasers examined was a profusion of long straight black lines as shown in fig. 1a.

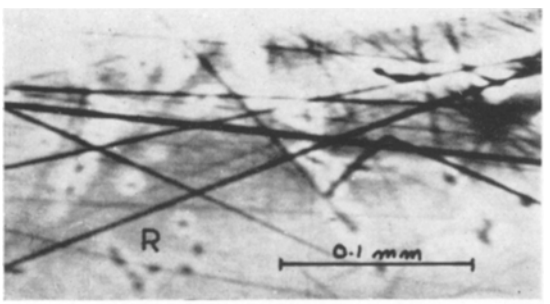

(a)

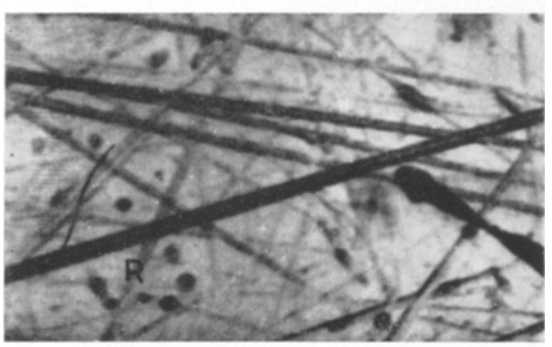

(b)

Figure 1(a) SEBECC micrograph of an area of a mirror face of a GaAs laser diode. (b) Optical micrograph of the same area after etching.

Some diodes also contained areas in which there appeared black dots and lines each of which was surrounded by a white region of constant width. Examples are shown in a ring marked R in fig. 1a and in fig. 2. The AB etch made both types of defect visible in optical micrographs, such as fig. 1b, of the originally smooth and featureless mirror faces. This indicates that the dark lines are subsurface damage produced during mechanical polishing. The rows of dislocation half-loops that constitute this type of damage have recently been seen in GaAs by transmission electron microscopy [15, 16]. The fact that the white-haloed dark areas are revealed by the etch, as shown at R in fig. 1b, is consistent with these features, being a Te segregation phenomenon. Some transmission electron microscope evidence of variation of etch rate with Te concentration in GaAs was obtained recently [17].

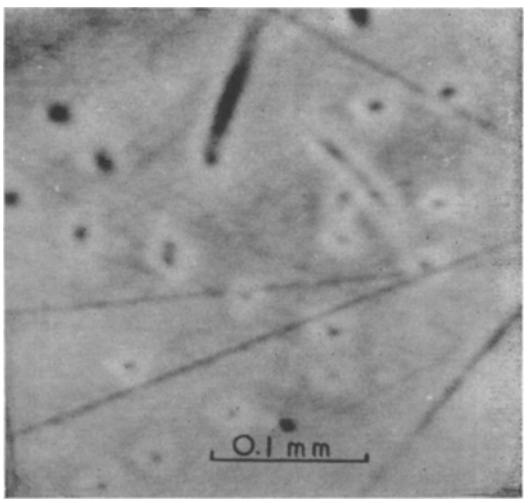

Figure 2 SEBECC micrograph showing white-haloed dark areas that probably represent the segregation of the Te dopant.

If the white haloes in fig. 2 are due to segregation by diffusion of the Te during the heat-treatment involved in the diffusion of Zn into the GaAs, then $L = (Dt)^{\frac{1}{2}}$. Here L is the diffusion length, D the diffusion coefficient of Te in GaAs at 850° C, and t is the annealing time. As can be seen in fig. 1a, L was found to be about 0.01 mm and t was 2½ h, giving $D = 10^{-10}$ cm²/sec. This value for D does not appear unreasonable in relation to what is known of the diffusion coefficients of other impurities in GaAs [18].

*Address: Baldock, Herts, UK

3.2. Factors affecting Visibility

Fig. 3 is a plot of the amplified signal from the two contacts versus distance during a line scan across the junction. The sharp local variations in the curve well away from the p-n junction peak are responsible for defect contrast in SEBECC micrographs.

Somewhere above the top of the peak in fig. 3 the signal strength becomes greater than the amplifier will accept. The range of signal strengths which the amplifier can handle is adjustable in the JEOL microanalyser. The result of changing the amplifier range is illustrated in fig. 4. Defects are only visible when the relative variation in the amplified video signal strength is sufficiently large and the (average) brightness on the CRO used for final display is suitably adjusted. Two extreme cases exist. Firstly the range to amplifier cut-off could be maximised so that the width of the plateau at the top of the peak was minimised, as in fig. 4a, and made to correspond to a narrow region across the p-n junction. Adjustment of the CRO screen brightness could then be made so that the only thing visible on the screen was a bright band corresponding to the display of the plateau of curves like that in fig. 4a. Such an image of a p-n junction region is marked J-J in fig. 5a. It was found useful to record, by double exposure on a photograph of the CRO screen, a second physically distinct type of scanning electron micrograph of the specimen. That so recorded in in fig. 5a is a secondary electron image or SEM micrograph. This shows dirt particles (the bright areas), and topographical features such as the defect marked D which appears to correlate with one of the kinks in the position of the p-n junction in the region marked K in fig. 5a. The second extreme case arose when the range of the amplifier was minimised as in fig. 3 (or 4c) so as

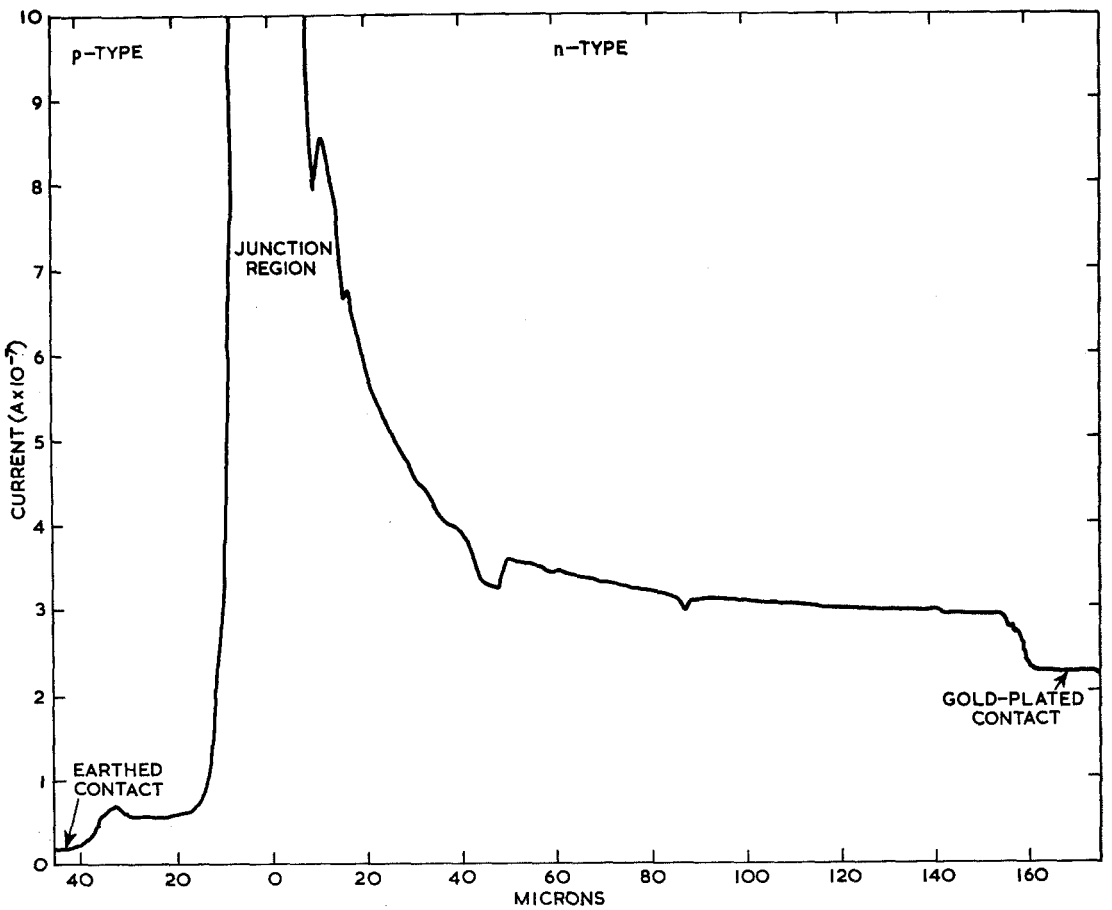

Figure 3 Signal strength versus distance in a line scan across a laser p-n junction.

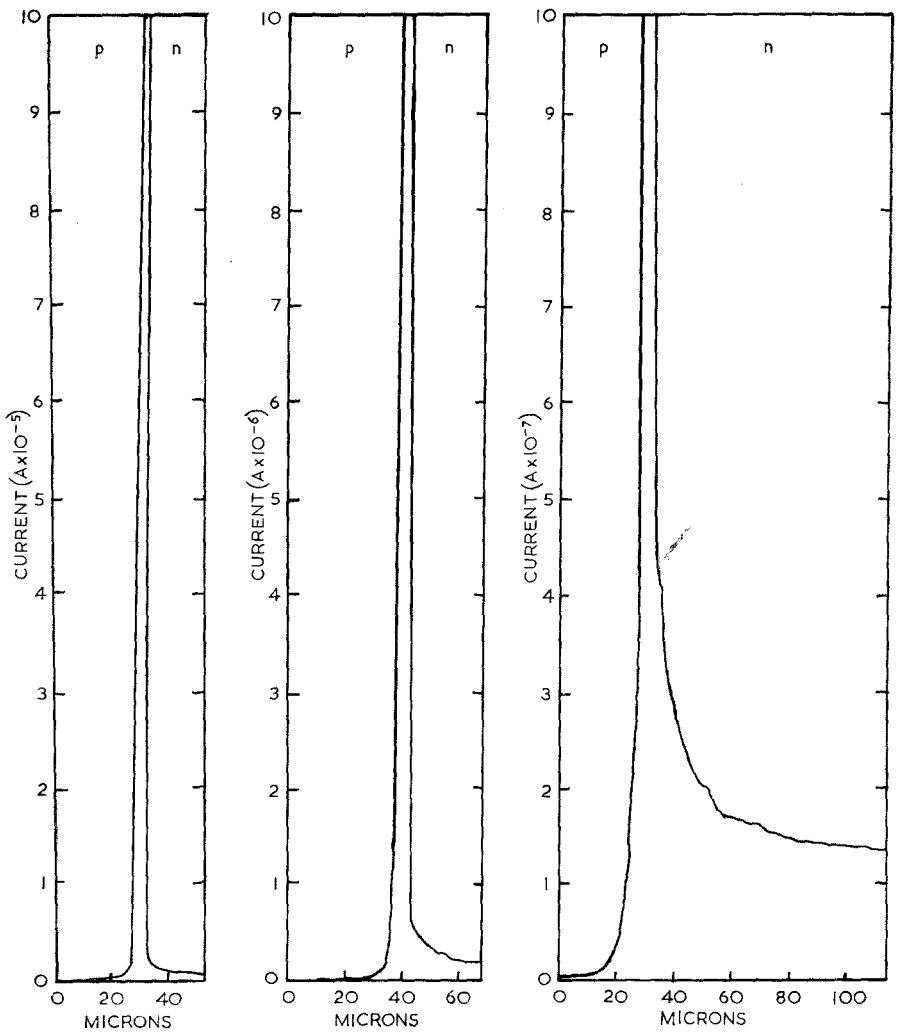

Figure 4 Signal strength versus distance for a line scan and a series of decreasing settings of the video amplifier range.

to maximise the relative signal variation due to defects. Turning up the brightness on the final display CRO then made defects visible over the whole of the Fabry-Perot mirror face of the laser except in a wide region at the p-n junction. A SEBECC micrograph taken under these conditions is shown in fig. 5b. The defect D is again visible together with mechanical polishing scratches. A possible interpretation is that the defect D is a small-angle grain boundary. Grain boundary segregation would result in a local hardness different from that of the remainder of the diode, and during polishing topographical relief as observed in fig. 5a would develop. Small angle boundaries promote diffusion and could therefore produce local deviations from planarity in the p-n junctions as seen at K in fig. 5a. In addition, an artefact is visible in fig. 5b, running roughly parallel to the p-n junction. This is a meandering double dark line. This arises during the recovery of the amplifier from its over-loaded state on each successive line scan. That is, as the beam passes out of the p-n junction region and down off the plateau at the top of the peak of figs. 3 and 4, spurious lines are generated on the micrograph. This was confirmed by rotating the specimen so that the direction of the electron beam scanning was reversed. When the scanning took place in the upward direction instead of downwards as in fig. 5b, the dark lines appeared on the other side of the p-n junction, that is at the top of the micrograph. The number of these dark lines: zero, one, or two, was also found to depend upon the operating conditions. The microanalyser conditions which affected this type of artefact were the electron beam accelerating voltage, the video amplifier range value, and the value of the

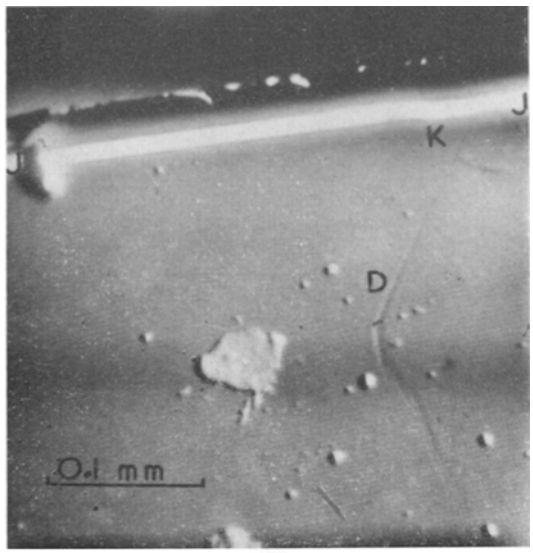

(a)

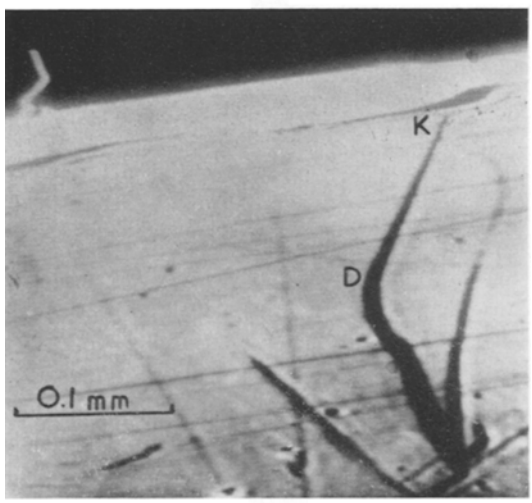

(b)

Figure 5 (a) Double exposure showing superposed a SEBECC image of the p-n junction region as a bright line J-J, and a secondary electron (SEM) micrograph of the surface showing dirt particles and a topographical feature D correlating with a kink in the p-n junction in the region K. (b) SEBECC micrograph (of the same diode) in which defect visibility has been maximised.

video amplifier "suppression". The suppression value is the magnitude of a reverse DC current applied to shift the signal zero, and thus to move the curves of 3 and 4 up or down relative to the range of signal strengths accepted by the amplifier.

3.3. The Role of the Defects in Laser Action

As is argued in detail elsewhere [17], the elongated dark areas surrounded by white haloes, that is large, linear, segregated volumes, are one of the few types of defects with the geometrical characteristics required to promote filamentary or spotty laser emission.

Small-angle boundaries may affect diffusion rates and produce non-flat p-n junctions [13]. The defect marked D in fig. 5a may be such a boundary. It is known that in general this results in diodes with very high thresholds or in diodes that do not lase [17].

The subsurface damage visible in figs. 1, 2, and 5b does not correlate with laser emission patterns at all. It must therefore be concluded that this type of defect has little or no effect on laser behaviour.

Acknowledgements

We would like to thank Dr D. L. Riley and Mr N. G. Ware for their help with the microanalyser, Professor J. G. Ball for the provision of research facilities, and the Ministry of Defence for financial support.

References

1. D. F. KYSER and D. B. WITTRY, "The Electron Microprobe", edited by T. D. McKinley, K. F. J. Heinrich, and D. B. Wittry (Wiley, New York, 1966) pp. 691–714.
2. *Idem*, *J. Appl. Phys.* **35** (1964) 2439.
3. *Idem*, *ibid* **36** (1965) 1387.
4. D. B. WITTRY, *Appl. Phys. Letters* **8** (1966) 142.
5. D. B. WITTRY and D. F. KYSER, *J. Phys. Soc. Japan* **21** Suppl. (1966) 312.
6. H. C. CASEY and R. H. KAISER, *J. Electrochem. Soc.* **114** (1967) 149.
7. H. C. CASEY, *ibid* **114** (1967) 153.
8. J. J. LANDER, H. SCHREIBER, T. M. BUCK, and J. R. MATHEWS, *Appl. Phys. Letters* **3** (1963) 206.
9. W. CZAJA and G. H. WHEATLEY, *J. Appl. Phys.* **35** (1964) 2782.
10. W. CZAJA and J. R. PATEL, *ibid* **36** (1965) 1476.
11. W. CZAJA, *ibid* **37** (1966) 918.
12. *Idem*, *ibid* 4236.
13. D. A. SHAW, K. A. HUGHES, N. F. B. NEVE, D. V. SULWAY, P. R. THORNTON, and C. GOOCH, *Solid State Electron.* **9** (1966) 664.
14. M. S. ABRAHAMS and C. J. BUIOCCHI, *J. Appl. Phys.* **36** (1965) 2855.
15. C. J. BUIOCCHI, *ibid* **38** (1967) 1980.
16. M. J. HILL, D. B. HOLT, and B. A. UNVALA, *J. Sci. Instr.* to be published.
17. M. J. HILL and D. B. HOLT, *J. Matls. Sci.* **3** (1968) to be published.
18. O. MADELUNG, "Physics of III-VI Compounds" (Wiley, New York, 1964) p. 245.